Arch. Metall. Mater. **67** (2022), 2, 507-519

DOI: https://doi.org/10.24425/amm.2022.137784

MOHD FIRDAUS OMAR[1,2*], MOHD MUSTAFA AL BAKRI ABDULLAH[1,2], SAM SUNG TING[1,2], B. JEŻ[3], M. NABIAŁEK[3], HAZIZAN MD AKIL[4], NIK NORIMAN ZULKEPLI[1], SHAYFULL ZAMREE ABD RAHIM[1], AZIDA AZMI[2]

INFLUENCE OF FILLER SURFACE MODIFICATION ON STATIC AND DYNAMIC MECHANICAL RESPONSES OF RICE HUSK REINFORCED LINEAR LOW-DENSITY POLYETHYLENE COMPOSITES

Filler surface modification has become an essential approach to improve the compatibility problem between natural fillers and polymer matrices. However, there is limited work that concerns on this particular effect under dynamic loading conditions. Therefore, in this study, both untreated and treated low linear density polyethylene/rice husk composites were tested under static (0.001 s^{-1}, 0.01 s^{-1} and 0.1 s^{-1}) and dynamic loading rates (650 s^{-1}, 900 s^{-1} and 1100 s^{-1}) using universal testing machine and split Hopkinson pressure bar equipment, respectively. Rice husk filler was modified using silane coupling agents at four different concentrations (1, 3, 5 and 7% weight percentage of silane) at room temperature. This surface modification was experimentally proven by Fourier transform infrared and Field emission scanning electron microscopy. Results show that strength properties, stiffness properties and yield behaviour of treated composites were higher than untreated composites. Among the treated composites, the 5% silane weight percentage composite shows the optimum mechanical properties. Besides, the rate of sensitivity of both untreated and treated composites also shows great dependency on strain rate sensitivity with increasing strain rate. On the other hand, the thermal activation volume shows contrary trend. For fracture surface analysis, the results show that the treated LLDPE/RH composites experienced less permanent deformation as compared to untreated LLDPE/RH composites. Besides, at dynamic loading, the fracture surface analysis of the treated composites showed good attachment between RH and LLDPE.

Keywords: Silane coupling agents; Strain rate; Universal testing machine; Split Hopkinson Pressure Bar; Strain rate sensitivity

1. Introduction

Natural fiber-reinforced polymer composites have greatly gained attention and interest among materials scientists and engineers in recent years due to its prominent mechanical properties and environmental advantages such as renewability and biodegradability [1]. One of the most promising bio-based polymers that have attracted many researchers in manufacturing thermoplastic polymer composites is linear low-density polyethylene (LLDPE). LLDPE has good mechanical properties and it is widely implemented in polymeric industry. Some of the products produced from LLDPE are grocery bags, heavy duty shipping sacks, agricultural films, pipes, liners for consumers, landscaping ties and compost bins [2]. Besides, the low processing temperature (below 160°C) of LLDPE makes composites fabrication possible without partial melting or annealing of the filler [3].

Nowadays, the addition of fillers into the polymer matrix is a fast and cheaper method to modify the properties of the neat polymer [4]. Among many types of fillers, natural fillers have a number of techno-ecological advantages over synthetic fillers due to their renewable nature, abundant resources, very low cost, recyclability, environmental-friendliness and non-abrasiveness to processing equipment [5].The use of natural filler derived from agricultural waste such as banana, bread-fruit, coconut shell, coir, jute, hemp, sugarcane bagasse, rice straw, palm oil leaves, sawdust, bamboo and rice husk (RH) can be used to reinforce thermoplastic to produce bio-composites[6]. RH is one of the major agro-waste products, which contains cellulose (25 to 35%), hemicelluloses (18 to 21%), lignin (26 to 31%), silica (15 to 17%), soluble (2 to 5%), and moisture (7.5%) [7]. Besides, most of rice husks are used as a bedding material for animal, land filling and the waste are burned. Therefore, the use of rice husks and its derivatives in

[1] UNIVERSITI MALAYSIA PERLIS (UNIMAP),CENTRE OF EXCELLENT GEOPOLYMER & GREEN TECHNOLOGY (CEGEOGTECH), PERLIS, MALAYSIA
[2] UNIVERSITI MALAYSIA PERLIS (UNIMAP), FACULTY OF CHEMICAL ENGINEERING TECHNOLOGY, PERLIS, MALAYSIA
[3] CZĘSTOCHOWA UNIVERSITY OF TECHNOLOGY, FACULTY OF MECHANICAL ENGINEERING AND COMPUTER SCIENCE, 42-200 CZĘSTOCHOWA, POLAND
[4] UNIVERSITI SAINS MALAYSIA, SCHOOL OF MATERIALS AND MINERAL RESOURCES ENGINEERING, PULAU PINANG, MALAYSIA

* Corresponding author: firdausomar@unimap.edu.my

the production of thermoplastic polymer composites is attracting much attention and has become one of the most important aspects of the industry to reduce environmental pollution problems [4]. The main purpose of using RH as filleris due to cost reduction as the cost of bio-sourced and biodegradable polymers is still high. However, like other natural fillers, RH has properties such as high hydrophilic due to the presence of hydroxyl groups on the RH surface. Furthermore, the existence of non-cellulosic components such as lignin and wax may prevent RH from having a good interfacial adhesion with hydrophobic thermoplastics in composites [8]. Therefore, various chemical treatments for RH were performed by previous researchers in order to increase the compatibility between RH and polymer matrices [9].

Many researchers have investigated the surface modification of natural fillers and their subsequent characterization in composites. The examples of chemical treatments used are silane treatment, alkaline treatment, acetylation treatment, benzoylation treatment, peroxide treatment, maleated coupling agents, sodium chlorite treatment, acrylation and acrylonitrile grafting, stearic acid treatment and permanganate treatment [10]. Silane is believed to become the most prominent coupling agent that has been widely used in composites and adhesive formulations [11]. Besides, silane coupling agents also have three main advantages, which are: (i) they are commercially available in a large scale; (ii) at the one end, the bear alkoxysilane groups of reacting with OH- rich surface, and (iii) at the other end, they have a large number of functional groups which can be tailored as a function of the matrix to be used. Additionally, it also has good compatibility between the reinforcing element and the polymer matrix or covalent bonds between them [12].

A coupling agent is a chemical that functions at the interface to create a chemical bond between the reinforcement and matrix. It improves the interfacial adhesion when one end of the molecule is tethered to the reinforcement surface and the functionality at the other end reacts with the polymer phase [11]. It can be observed that γ-aminopropyltriethoxy silane (named APS) is widely applied by natural filler reinforced polyethylene [13]. Therefore, the use of a silane coupling agent can improve the interfacial adhesion between the polar hydrophilic RH and the non-polar hydrophobic LLDPE polymeric chains [14].

From previous findings, it has been reported that up to a certain filler loading, the mechanical properties of particulate natural filler–reinforced composites tend to decrease down to a certain extent [15-19]. Besides, the mechanical properties of composites also give significant effects under both static and dynamic loading. To overcome these problems, RH surface was chemically modified using a silane coupling agent that improves its suitability as a reinforcing material with LLDPE. Besides, RH was functionalized with a silane-based coupling agent that may react with both filler and the matrix during the mixing process that could improve the interfacial adhesion between the filler and the matrix. From previous findings, it has been reported that both untreated and treated filler had given significant effect to the mechanical properties of particulate natural filler-reinforced composites [20,21]. Unfortunately, this kind of effect was never correlated with the mechanical performance of polymer composite under critical condition such as dynamic loading. From published literatures, none of previous works have specifically reported the effect of silane treatment on the dynamic mechanical properties of particulate natural filler-reinforced composites. To overcome the lack of information in this area, this paper has been purposefully design to investigate and analyse the capability of untreated and treated LLDPE/RH composites under various loading rates especially dynamic loading. To achieve the aim of this study, this experiment was designed to investigate the effect of silane coupling agent on the mechanical properties of LLDPE/RH composites under static and dynamic loading using universal testing machine (UTM) and SHPB equipment. Besides, the sensitivity towards strain rate of both untreated and treated LLDPE/RH composites was also calculated using a specific equation. The fractographic analysis was also demonstrated to investigate the failure mechanism of untreated and treated LLDPE/RH composites under dynamic loading rates.

2. Experimental Detail

2.1. Material

LLDPE was supplied by Lotte Chemical Titan Holding Sdn. Bhd in pellet form, used as polymer matrix for the composites. The density, the melt flow index and the melting point of used LLDPE are approximately 0.922 g/cm^3, 2 g/10 min and 160°C, respectively. RH used as filler was obtained from Padi Bernas Nasional Berhad (BERNAS) and was ground to obtain the particle size of approximately 125 μm. Besides, γ-aminopropyltriethoxy silane (named APS) was purchased from Lotte Chemical Titan Holding Sdn. Bhd in liquid form. The present chemical grafting that involves functionalized γ-aminopropyltriethoxy silane coupling agents is shown in Figure 1.

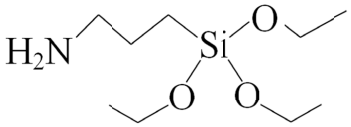

γ-Aminoproyltriethoxysilane
APS

Fig. 1. The chemical structure of silane coupling agents used in this study

2.2. Silane treatment procedure

1 wt. % of silane (weight percentage compared to the RH) was dissolved in a mixture of water/ethanol (30/70 volume, respectively). The pH of the solution was adjusted to 4 with acetic acid using pH meter. Then, the solution was stirred continuously for 30 min. After that, 25 g of RH were soaked in solution for 3 hours and washed with distilled water. The treated RH was filtered and dried in oven at 60°C for 24 hours. Similar procedures were repeated for 3, 5, and 7% (weight percentage) of silane.

2.3. Characterization Methods

2.3.1. Fourier Transform Infrared Spectroscopy (FTIR)

FTIR was used to determine changes in chemical functional groups of untreated and treated RH. The spectra range chosen was from 4000 to 450 cm^{-1} using a FTIR spectrometer (Perkin Elmer). Before testing, a powder form of the untreated and treated RH was mixed with KBr powders and cold-pressed into a suitable disk.

2.3.2. Field Emission Scanning Electron Microscopy (FESEM)

The surface morphologies of untreated RH, treated RH and fracture surface of the dynamic loadings treated composites were coated with platinum and then examined using FESEM (ZEIZZ).

2.4. Fabrication of polymer composites

2.4.1. Compounding process

LLDPE pallets, untreated and treated RH were mixed by BENCHOP twin screw extruder. The speed rate was kept at 60 rpm with temperature of 160°C. Untreated RH was run first and followed by treated RH with five different weight percentages of silane (1, 3, 5 and 7 wt %). Untreated and treated RH was dried at 60°C for 3 hours in oven to remove the moisture contents before being compressed.

2.4.2 Compression molding process

The specimens were compression moulded in hydraulic hot press using a button mould with 12 mm (diameter) × 27 mm (width). Firstly, approximately 2.1 gram of composites was weighed and placed for each button mould cavity. After that, the compounded composites were compressed with specific timing that involved pre-heating for 20 minutes followed by compressing for 10 minutes and cooling for 10 minutes at 160°C. Then, the moulded composites were cut using a bench saw into 12 mm (diameter) × 18 mm (length) and 12 mm (diameter) × 6 mm (length) for both static and dynamic mechanical testing respectively.

2.5. Mechanical tests

2.5.1. Static compression testing

For static testing, the compression specimen was compressed under a constant crosshead speed of 1.08 mm/min, 10.8 mm/min and 108 mm/min; which corresponds to strain rates of 0.001 s^{-1}, 0.01 s^{-1} and 0.1 s^{-1}, using a Universal Testing Machine. As a precaution step, a thin film of lubricant was pasted onto both ends of the compression specimens to eliminate the needles effect (i.e., frictional effect) during the test. Five measurements were taken for each strain rate in order to quantify the average behaviour of the tested specimens.

2.5.2. Dynamic compression testing

The dynamic compression test was performed using the compression Split Hopkinson Pressure Bar (SHPB) equipment. Usually, the SHPB equipment consists of a striker bar, an incident bar, a transmission bar, and a sample placed between the incident and transmission bars as shown in Figure 1. When a gas gun launches the striker bar at the incident bar, the impact causes an elastic compression wave to travel in the incident bar towards the sample. When the impedance of the sample is less than that of the bars, an elastic tensile wave is reflected into the incident bar and an elastic compression wave is transmitted into the transmission bar [22].

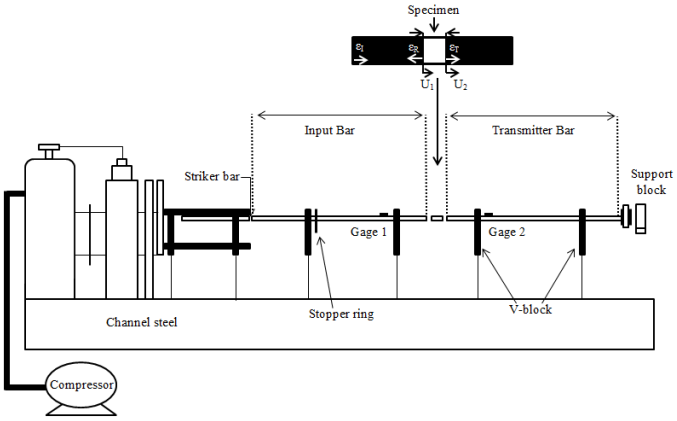

Fig. 2. The schematic diagram of the split Hopkinson pressure bar equipment

Generally, during SHPB operation, a striker bar is launched at a speed to collide with the incident bar, generating an incident strain pulse, ε_I, that propagates along the bar until it arrived at the specimen. At this point, acoustic impedance mismatch between bar and specimen material results in a portion of the pulse being reflected back along the incident bar, producing a strain ε_R, while some of the pulse is transmitted through the specimen ε_T [23]. The histories of stress, strain and strain rate during compression SHPB testing were calculated based on the strain measured on the incident and transmitter bars. The equations involved are shown as follows:

$$\sigma_S(t) = E\frac{A_b}{A_s}\varepsilon_r(t) \tag{1}$$

$$\varepsilon_S = -\frac{2C_0}{L}\int_0^t \varepsilon_r(t)\,dt \tag{2}$$

$$\dot{\varepsilon}_S = \frac{d\varepsilon(t)}{dt} = \frac{-2c}{L}\varepsilon_R(t) \quad (3)$$

Where A, E and c ($= E/\rho^{1/2}$, ρ is mass density of the bar) are cross-sectional area, Young's modulus and wave velocity of the bars, respectively. L and A_s refer to the length and cross-sectional area of the sample. $\varepsilon_r(t)$ and $\varepsilon_t(t)$ are the recorded axial strains of the reflected pulse and transmitted pulse, respectively, measured in reflected and transmitted bar as function of time. The derivation of equation (1)-(3) is closely related with the following assumptions and idea [24]:

1. The propagation of wave in the Hopkinson bars is well-approximated by one-dimensional theory where the wave dispersion is totally negligible.
2. The stress and strain states in the specimen are homogeneous.
3. The friction and radial inertia effect are negligible.

3. Results and Discussion

3.1. FTIR analysis

The presence of the silane onto the RH surface after the chemical treatment was assessed using FTIR spectroscopy. The resultant spectra for treated RH and untreated RH are compared in Figure 3. From the figure, the peak 3412 cm^{-1} represents the –OH stretching vibration due to hydroxyl group in the RH. Besides, the peak at 1728 $cm^{-1}$is also present in both treated and untreated RH. This peak is a C = O that represents the carboxylic group from hemicellulose [25]. In addition, the peak at 1514 cm^{-1} also exists in both treated and untreated rice husk. This peak indicated C = C stretching from lignin that still remains before and after the silane treatment.

By comparing the FTIR spectra, a peak at 796 cm^{-1} appeared for both untreated RH and treated RH. As RH contains 14.5% of silica, it will hide bands assigned to the stretching vibration of Si-O-C where a reaction occurred between the silane agent and the RH surface [8]. Furthermore, this stretching vibration of Si-O-C that is related to silane overlaps with silica content in RH that causes the characteristics of silane could not be detected by FTIR spectra. Besides that, a new peak appeared at 1098 cm^{-1} after the treatment. This peak is a Si-O-Si stretching vibration that formed after $CH_2CH(O)CH_2$-$O(CH_2)_3SiO$- group has been grafted onto the cellulose molecules [26]. The process can be described as follows:

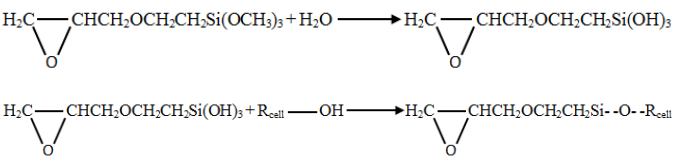

From the peak at FTIR spectra in Figure 3, it can be concluded that cellulose, hemicellulose and lignin do not change in the rice husk after the treatment but a new chemical bond has been found in the rice husk after the treatment. The FTIR findings also confirm the presence of silane in treated RH after the silane treatment, validating the SEM analysis.

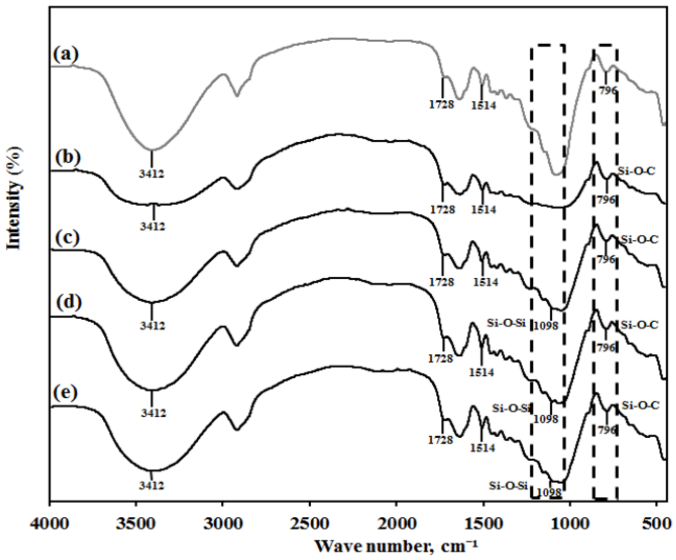

Fig. 3. Comparison of FTIR spectra obtained for (a) untreated RH, (b) 1% silane-treated, (c)3% silane-treated, (d)5% silane-treated and (e) 7% silane-treated

3.2. SEM analysis

Scanning electron microscopy (SEM) provides an excellent technique for examining the surface morphology of untreated and treated rice husk fillers. It is expected that the surface morphology of untreated rice husk will be different to the treated rice husk particularly in terms of their level of smoothness and roughness [26]. It is important to study the filler surface morphology that provides vital information on the level of interfacial adhesion that would exist between the filler and the matrix later when used as reinforcement filler with and without treatment.

For standardization, all micrographs of rice husk are taken under 500× magnification. Figure 4 (a) shows the SEM micrograph of untreated rice husk filler. Clearly, the impurities were observed on the surface of untreated filler. On the other hand, Figure 4 (b) shows only a thin layer coated around the rice husk filler. It indicates that 1% of silane was not enough to coat the filler with the matrix. Besides, Figure 4(c) also shows a thin layer of coating and a few crackings on the rice husk surface. Thus, it indicates that 3% of silane also was not good enough for coupling matrix with fillers. Figure 4(d) shows the SEM micrograph of 5% of silane. It can be observed that a smooth thin layer coating around the filler with a good cracking around the rice husk filler. This finding is in line with the one that has been documented by Gonzalez and his co-workers, where they recorded that 5% silane weight percentage was the optimum concentration for their natural fiber-reinforced composite specimen [27]. Besides, Figure 4(e) shows the deterioration of rice husk surface with more cracking. As compared to the 5% of

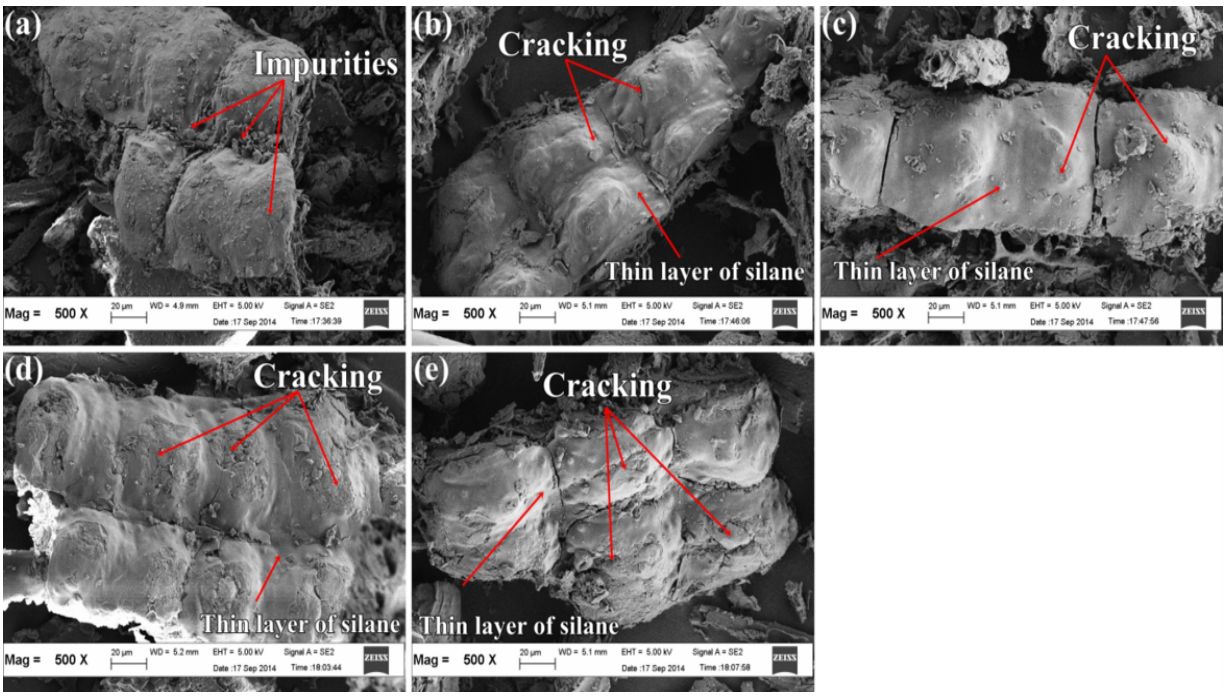

Fig. 4. SEM images of the surfaces of (a) untreated RH, (b) 1% silane-treated, (c) 3% silane-treated, (d) 5% silane-treated and (e) 7% silane-treated RH

silane treatment, the rice husk surface looks jagged and broken. So, it can be pre-concluded that the 5% of silane showed the best chemical surface treatment of silane coupling agent. Similar observation has been found by Lu et al. [26], where they clarified that a tiny thin film appears on the cellulose surface after silane modification, which was ascribed to the coupling agent.

3.3. Effect of silane coupling agent on mechanical properties of untreated and treated LLDPPE/RH composites under a wide range of strain rates

3.3.1. Strength properties

Strength properties are the best statistical indicators that can be used to evaluate the performance of materials. Therefore, the ultimate compressive strength (UCS) of untreated and treated LLDPE/RH composites under a wide range of strain rate loading is demonstrated in Figure 5. From the graph in Figure 5, it can be clearly seen that treated composites have the highest compressive value compared to untreated composites under both static and dynamic loading. For both static and dynamic loading, the ultimate compressive strength begins to increase significantly at silane concentration of around 3% and reaches its maximum value at silane concentration of around 5%. The increase in UCS of treated composites is due to the improved adhesion and effective wetting of the filler by the matrix [14]. This finding is in line with the work reported by Huda et al. [28], who state that silane coupling agents can minimize the incompatibility between the polymer matrix and the filler by improving the interaction at the LLDPE/RH interface.

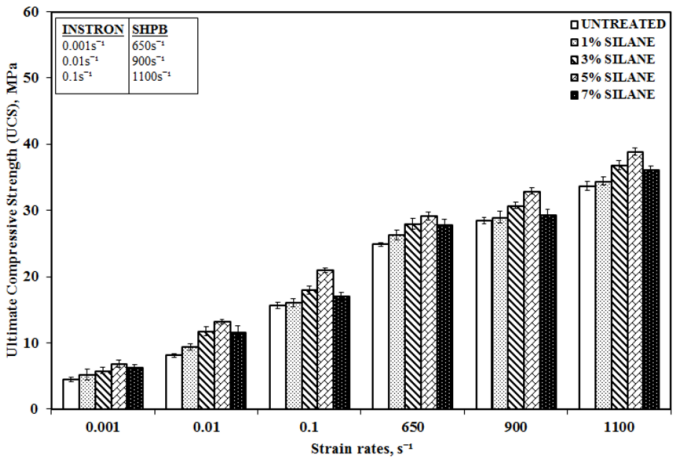

Fig. 5. The ultimate compressive strength (UCS) of the untreated LLDPE/RH and the treated LLDPE/RH composites under various loading rates

Theoretically, the reaction of silane with lignocellulosis RH could be interpreted by the illustration of chemical modification in Figure 6. Firstly, silane was hydrolyzed in water/ethanol solutions to produce silanol and alcohol group. Secondly, the hydrolyzed alkoxysilanol could be absorbed into the surface of the cellulosic parts. After that, a condensation reaction occurs between the silanol group (Si-OH) and the hydroxyl group on the cellulosic surface parts. With this reaction, a covalent bond was formed through an ether linkage between the RH surface and the silanol groups with water removal. The remaining silanol groups were capable of hydrogen bonding or condensing with adjacent silanol groups forming –Si-O-Si- link. Lastly, the hydrophobic part of the silane on the cellulosic treated RH surface

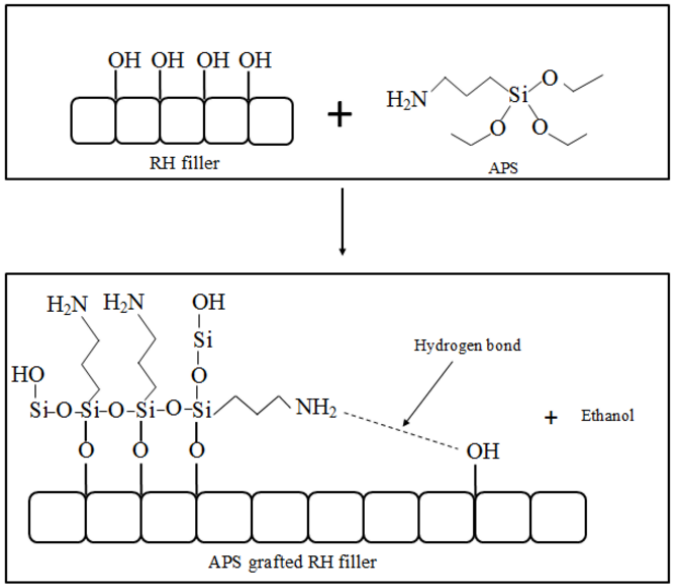

Fig. 6. The illustration of APS silane molecules on RH filler surfaces [29]

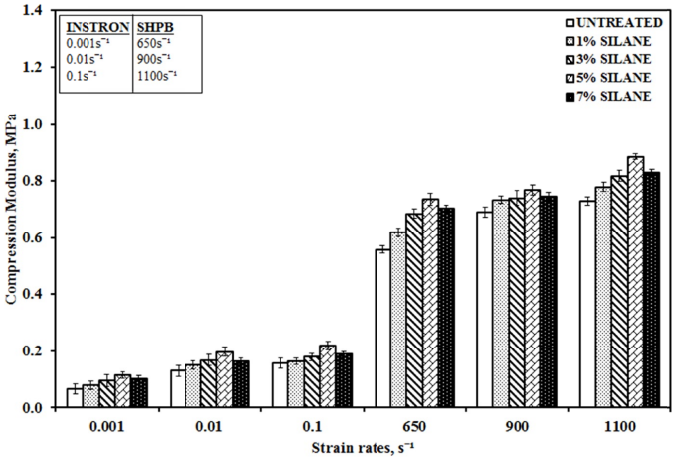

Fig. 7. The compression modulus of the untreated LLDPE/RH and the treated LLDPE/RH composites under various loading rates

could chemically bound through a covalent bond or interact with hydrogen bond. The possibility of hydrogen bonding was higher due to the presence of nitrogen in amino group. Thus, hydrophilic part (treated RH fillers) and hydrophobic part (LLDPE) could be coupled together with the silane that functions as bridge between them. With this mechanism, the adhesion between treated RH and LLDPE was improved and it is possible for better stress transfer to occur from matrix to RH during compounding, thus improving the UCS of the treated composites [14]. The presence of this remarkable silane bridge between RH filler and LLDPE composites also improve their strength properties at higher strain rate conditions (higher deformation rates) by reducing the discontinuity mechanism in form of debonding. This will indirectly lead to an increase in compressive strength especially for treated RH with better stress transfer mechanism. However, due to the excessive damage to the RH surface at 7% of silane treatment, the strength properties were seen to deteriorate which somehow were still higher than that of untreated LLDPE/RH composites. This may be attributed to the decrease in inherent strength of the single RH particle due to removal of its substances.

3.3.2. Stiffness properties

The compression modulus of untreated and treated LLDPE/RH composites under various loading rates is shown in Figure 7. The bar graph in Figure 7 clearly shows that the relationship between strain rate and compression modulus was almost identical under both static and dynamic loading rates where treated specimen shows higher stiffness properties than that of its counterpart (untreated specimen). The highest compression modulus was recorded by 5% silane-treated LLDPE/RH composites for both static and dynamic testing. For example, at strain rate of 0.001 s^{-1} and 1100 s^{-1}, the compression modulus for untreated LLDPE/RH composites is 0.0067 GPa and 0.730 GPa. Meanwhile, the compression modulus for 5 % treated-composites was found increase to 0.116 GPa and 0.886 GPa.

This increment in compression modulus was due to the silane treatments that enhance the filler/matrix adhesion and increase the stiffness of treated composites [30]. According to Demir et al. [31], the increase in the modulus is due to the silane treatment that can be attributed to the better disparity in the hydrophobic matrix and also better filler/matrix adhesion. Thus, the improved adhesion increases the restriction to deformation capacity of the matrix in the elastic area that is increasing the modulus. Theoretically, it is well-known from the chemistry of coupling agents on glass fibers that the efficient stress transfer from a matrix to a filler that has been treated with a coupling agents gives the improvement in the modulus [31]. Similar finding has been reported by Maziad et al. [14], where they speculated that the modulus of the chemically treated composites exhibited higher modulus values than untreated composites due to the presence of a strong interface between the RH and matrix. Thus, the load transfer between the RH and matrix occurred through the strong RH/matrix interface that gives the modulus value of a well-bonded composite increase. Similar with strength properties, excessive removal of stiffer substances at 7% of silane treatment had slightly decreased the stiffness properties of tested LLDPE/RH composites. Yet, the compression modulus for treated LLDPE/RH composites with 7% of silane treatment is still higher than that of untreated LLDPE/RH composites.

3.3.3. Yield Behavior

Generally, the yield stress may be defined as the stress at which materials experience a major micro structural deformation [32]. It would be essential to determine the stress strain value at the yield point, so that we can identify the effect of silane treatment as well as strain rate towards the elastic deformation of LLDPE/RH composites at both static and dynamic loadings. Thus, the yield stress and yield strain of untreated and treated

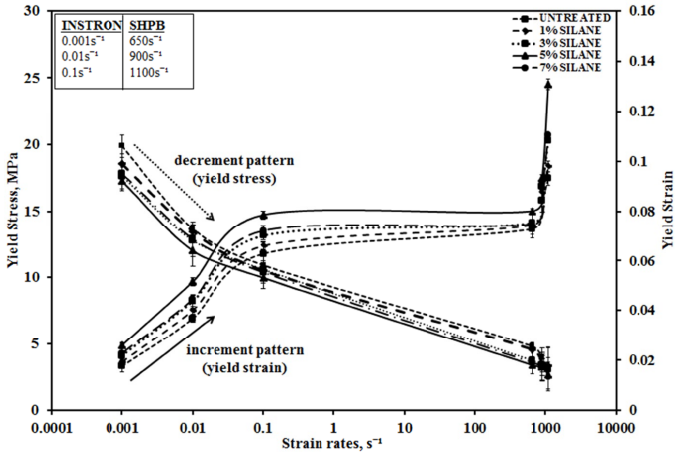

Fig. 8. The yield stress and the yield strain of the untreated and the treated LLDPE/RH composites under a wide range of strain rates

LLDPE/RH composites were obtained under various levels of strain rates, as shown in Figure 8. From Figure 8, it is clearly seen that the relationship between strain rate and yield stress is most similar under both static and dynamic loadings, where the yield stress increased up to 5% treated silane LLDPE/RH composites before it started to show reduced values. According to Parida et al. [33], the increment of yield stress value is due to the improvement of the interfacial adhesion between filler and matrix that is enhanced by silane coupling agent.

Another phenomenon was reported by Shanmugan et al. [34], who state that good filler matrix adhesion resulting from physical modification, such as formation of rough surface that occurs on the filler surfaces during chemical treatment, improved the yield stress of treated composites. On the contrary, the yield strain decreased with the increasing strain rates for both untreated and treated LLDPE/RH specimen. For both static and dynamic loading, the yield strain for 5%treated silane contributes the lowest value. It is believed that the difficulty of debonding and voiding (due to the remarkable silane bridge between RH and LLDPE) leads to composites brittleness (less deformation) as a result of the high yield stress and restriction of plastic flow [35]. All the information gathered from the effect of silane coupling agent on mechanical properties of LLDPE/RH composites are grouped together and summarized in TABLE 1.

TABLE 1

The overall properties of untreated LLDPE/RH composite and treated composites under various loading rates

LLDPE/RH with different filler content (%)	Strain rates (s^{-1})	Yield stress (MPa)	Yield strain (MPa)	UCS (MPa)	Compression modulus (GPa)
UNTREATED	0.001	3.3±0.4249	0.106±0.0085	4.45±0.356	0.067±0.0188
	0.01	6.9±0.2830	0.073±0.0028	8.13±0.277	0.131±0.0194
	0.1	11.79±0.9550	0.0583±0.0010	15.57±0.466	0.157±0.0167
	650	13.67±0.6647	0.0256±0.0107	24.9±0.283	0.558±0.0127
	900	15.8±0.8490	0.0211±0.0106	28.5±0.490	0.690±0.0181
	1100	17.45±0.4950	0.0172±0.0038	33.7±0.710	0.730±0.0143
1% SILANE	0.001	3.62±0.5012	0.0989±0.0039	5.18±0.821	0.079±0.0137
	0.01	7.52±0.3113	0.0719±0.0023	9.39±0.540	0.150±0.0145
	0.1	12.38±0.2444	0.0561±0.0019	16.10±0.589	0.165±0.0114
	650	13.96±0.3651	0.0243±0.0028	26.30±0.712	0.619±0.0136
	900	16.41±0.3279	0.0189±0.0045	28.99±0.857	0.735±0.0138
	1100	18.34±0.4007	0.0179±0.0013	34.44±0.575	0.780±0.0158
3% SILANE	0.001	4.1±0.2902	0.0951±0.0032	5.83±0.436	0.096±0.0206
	0.01	8.21±0.5201	0.0689±0.0054	11.78±0.727	0.169±0.0197
	0.1	13.16±0.3079	0.0554±0.0041	17.98±0.661	0.180±0.0131
	650	14.13±0.2601	0.0191±0.0045	28.00±0.804	0.685±0.0162
	900	16.89±0.2563	0.0179±0.0027	30.75±0.473	0.740±0.0262
	1100	20.32±0.1457	0.0165±0.0087	36.89±0.696	0.819±0.0192
5% SILANE	0.001	4.87±0.1387	0.0921±0.0037	6.83±0.520	0.116±0.0110
	0.01	9.68±0.2804	0.0641±0.0063	13.25±0.332	0.198±0.0172
	0.1	14.73±0.3024	0.0532±0.0042	20.98±0.359	0.220±0.0143
	650	15.02±0.179	0.0181±0.0012	29.19±0.638	0.736±0.0223
	900	17.51±0.2200	0.0173±0.0052	32.95±0.468	0.769±0.0189
	1100	24.53±0.3802	0.0141±0.0017	38.89±0.563	0.886±0.0101
7% SILANE	0.001	4.29±0.8003	0.0941±0.0053	6.33±0.471	0.103±0.0116
	0.01	8.35±0.3057	0.0682±0.0066	11.65±0.982	0.163±0.0114
	0.1	13.53±0.4258	0.0566±0.0020	17.10±0.510	0.189±0.0102
	650	14.06±0.7702	0.0120±0.0012	27.86±0.788	0.704±0.0106
	900	16.78±0.6750	0.0183±0.0065	29.33±0.842	0.745±0.0146
	1100	29.67±0.1361	0.0167±0.0083	36.20±0.455	0.832±0.0104

3.4. Effect of silane coupling agent on rate sensitivity of untreated and treated LLDPE/RH composites under a wide range of strain rates

3.4.1. Strain rate sensitivity and thermal activation volume

In this study, the strain rate sensitivity has become our main consideration due to the fact that every material will react differently under various loading rates. This information is also crucial in order to predict the magnitude of changes for tested material under different strain rate conditions. With the value that is obtained from the strain rate sensitivity, each material can be compared to one another. Thus, the strain rate sensitivity was calculated using an established parameter which can be expressed as follows:

$$\beta = \frac{\sigma_2 - \sigma_1}{\ln\left(\dot{\varepsilon}_1 / \dot{\varepsilon}_2\right)} \bigg| \dot{\varepsilon}_2 > \dot{\varepsilon}_1 ,\ \varepsilon = 0.025 \tag{4}$$

Where, σ_1 and σ_2 is the flow stress at a fixed strain (in this case, the strain used was 0.025) under different strain rates. Besides, there is a significant relationship between the strain rate sensitivity and thermal activation volume of materials, as previously reported by Choi et al. [36]. Therefore, the derivation of thermal activation volume can be expressed by the following equation:

$$V^* = kT \left[\frac{\ln\left(\dfrac{\dot{\varepsilon}_2}{\dot{\varepsilon}_1}\right)}{\sigma_2 - \sigma_1} \right] = \frac{kT}{\beta} \tag{5}$$

Where, k is the Boltzmann Constant and T is the absolute temperature.

In summary, all calculated strain rate sensitivities and thermal activation volumes of untreated and treated LLDPE/RH composites under static and dynamic loadings are grouped in Table 2. From the results shown in Table 2, it can be seen that both untreated and treated LLDPE/RH specimens showed positive increment in strain rate sensitivity, with increasing strain rates, from static to dynamic regions. However, thermal activation volume shows a decrement pattern with an increasing strain rate.

At dynamic loading, the mobility of the molecular chain is restricted and it contributes to the lower thermal activation volume of both untreated and treated composites. Therefore, at static loading, the entanglement of the polymer chains increases with an increase in the thermal activation volume [37]. Thus, it can be seen that the filler treatment does not give any significant relationship with the rate of sensitivity and thermal activation volume of LLDPE/RH composites.

3.5. Post-damage Analysis

3.5.1. Physical Analysis

Figure 9(a), (b), (c), (d) and (e) show the photographs of untreated, 1% silane-treated, 3% silane-treated, 5% silane-treated and 7% silane-treated under different static loadings (0.001 s^{-1}, 0.01 s^{-1} and 0.1 s^{-1}) whereas Figures 10(a), (b), (c), (d) and (e) show the photograph of LLDPE/RH composites under dynamic loadings (650 s^{-1}, 900 s^{-1} and 1100 s^{-1}). The failure characteristics of tested composites were observed to be completely differ-

TABLE 2

The rate sensitivity and thermal activation volume of untreated and treated LLDPE/RH composites with different strain rates

LLDPE/RH with different filler content (%)	**Range of strain rates (s^{-1})**	**Classification**	$\beta = \frac{\sigma_2 - \sigma_1}{\ln\left(\dot{\varepsilon}_1 / \dot{\varepsilon}_2\right)}$ (MPa) $\dot{\varepsilon}_2 > \dot{\varepsilon}_1$ $\varepsilon = 0.025$	$V^* = kT\left[\frac{\ln\left(\frac{\dot{\varepsilon}_2}{\dot{\varepsilon}_1}\right)}{\sigma_2 - \sigma_1}\right] = \frac{kT}{\beta}$ (m^3) $\dot{\varepsilon}_2 > \dot{\varepsilon}_1$ $\varepsilon = 0.025$
UNTREATED	0.001 to 0.1	Static	0.2845	1.3256×10^{-20}
	0.1 to 650	Static to dynamic	2.1152	1.7830×10^{-21}
	650 to 1100	Dynamic	7.4132	5.0870×10^{-22}
1% SILANE	0.001 to 0.1	Static	0.1719	2.1927×10^{-20}
	0.1 to 650	Static to dynamic	1.8740	2.0124×10^{-21}
	650 to 1100	Dynamic	9.2189	4.0908×10^{-22}
3% SILANE	0.001 to 0.1	Static	0.1788	2.1089×10^{-20}
	0.1 to 650	Static to dynamic	1.7611	2.1415×10^{-21}
	650 to 1100	Dynamic	19.1918	1.9644×10^{-22}
5% SILANE	0.001 to 0.1	Static	0.2323	1.6231×10^{-20}
	0.1 to 650	Static to dynamic	1.9456	1.9383×10^{-21}
	650 to 1100	Dynamic	21.6692	1.7404×10^{-22}
7% SILANE	0.001 to 0.1	Static	0.1652	2.2834×10^{-20}
	0.1 to 650	Static to dynamic	1.9231	1.9611×10^{-21}
	650 to 1100	Dynamic	16.518	2.2831×10^{-22}

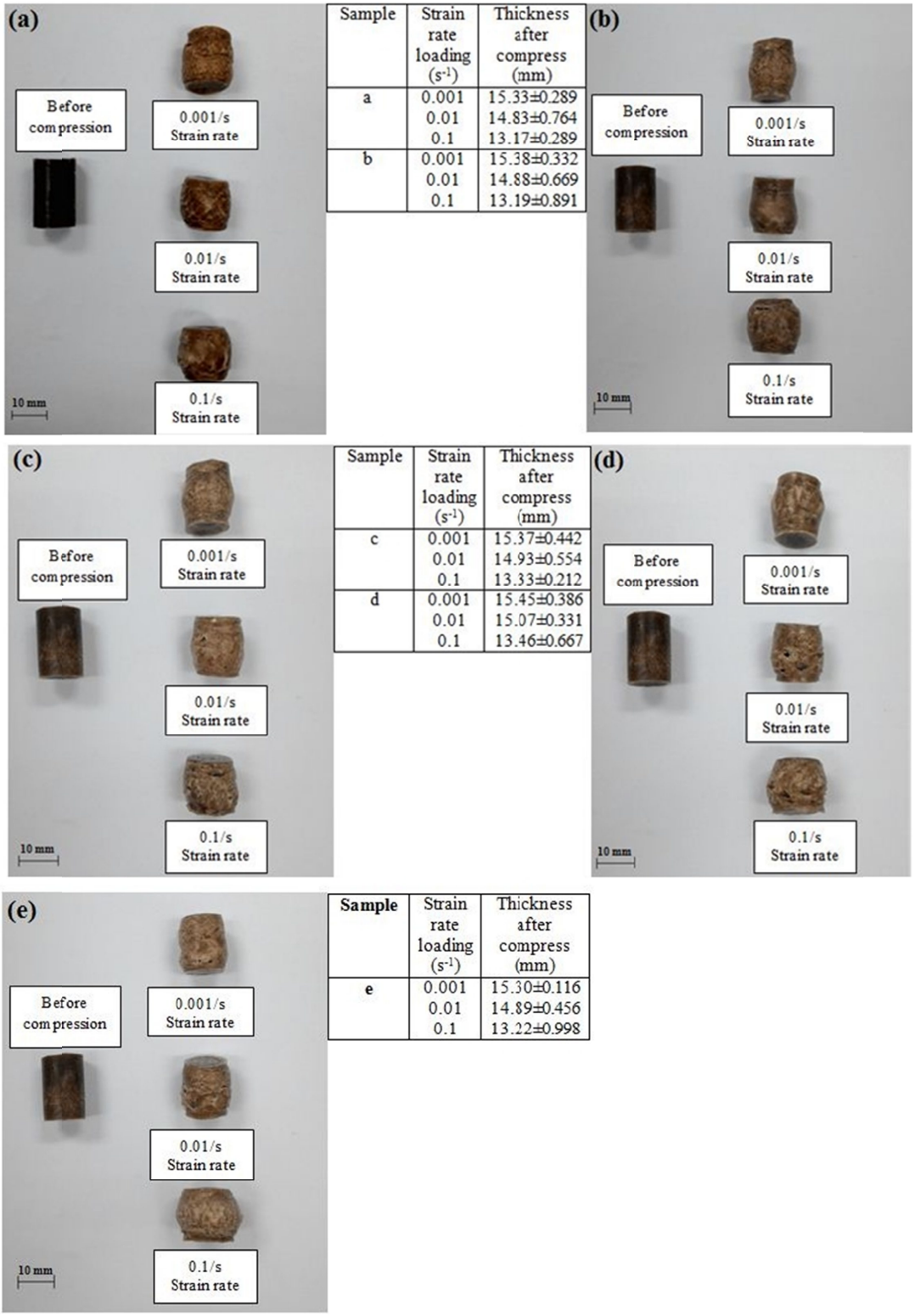

Sample	Strain rate loading (s^{-1})	Thickness after compress (mm)
a	0.001	15.33±0.289
	0.01	14.83±0.764
	0.1	13.17±0.289
b	0.001	15.38±0.332
	0.01	14.88±0.669
	0.1	13.19±0.891

Sample	Strain rate loading (s^{-1})	Thickness after compress (mm)
c	0.001	15.37±0.442
	0.01	14.93±0.554
	0.1	13.33±0.212
d	0.001	15.45±0.386
	0.01	15.07±0.331
	0.1	13.46±0.667

Sample	Strain rate loading (s^{-1})	Thickness after compress (mm)
e	0.001	15.30±0.116
	0.01	14.89±0.456
	0.1	13.22±0.998

Fig. 9. LLDPE/RH composites (a) untreated (b) 1% silane-treated (c) 3% silane-treated (d) 5% silane-treated and (e) 7% silane-treated at static loading loadings

ent between static and dynamic loading. From Figure 9, it can be seen that strain rate applied gives significant effect towards the deformation behavior of both untreated and treated LLDPE/RH composites. The increments of applied strain rate make the samples shorter (at specific applied load of 3 kN as shown in Figure 9. Thus, itis physically proven that untreated and treated LLDPE/RH composites experienced higher deformation rate with an increase of strain rate loading (under static condition).

Although the failure can be categorized under micro bulking phenomenon, no crack existed for both untreated and treated LLDPE/RH composites. It is believed that when a composite material is subjected to a compressive load, several major failure

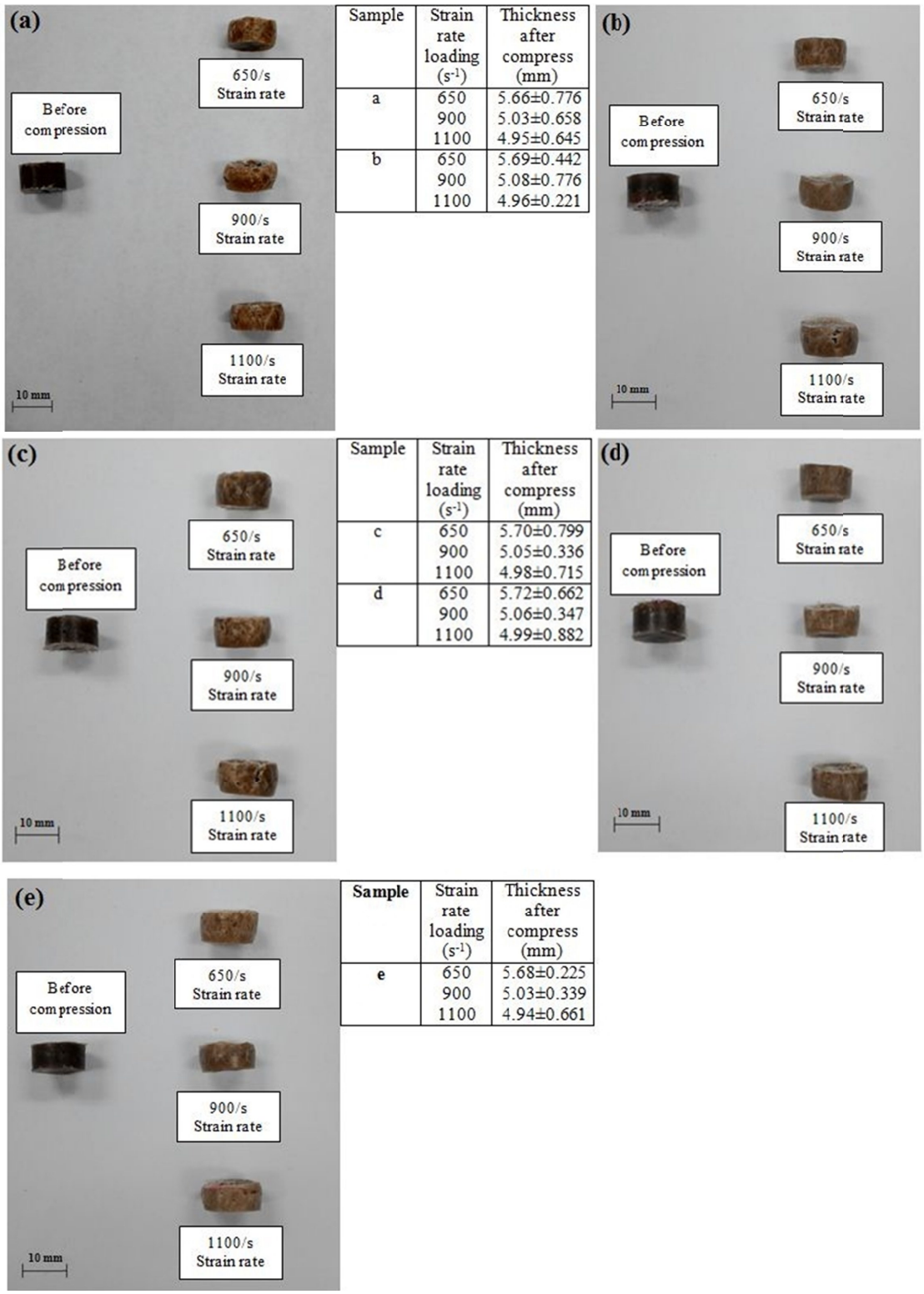

Sample	Strain rate loading (s^{-1})	Thickness after compress (mm)
a	650	5.66±0.776
	900	5.03±0.658
	1100	4.95±0.645
b	650	5.69±0.442
	900	5.08±0.776
	1100	4.96±0.221

Sample	Strain rate loading (s^{-1})	Thickness after compress (mm)
c	650	5.70±0.799
	900	5.05±0.336
	1100	4.98±0.715
d	650	5.72±0.662
	900	5.06±0.347
	1100	4.99±0.882

Sample	Strain rate loading (s^{-1})	Thickness after compress (mm)
e	650	5.68±0.225
	900	5.03±0.339
	1100	4.94±0.661

Fig. 10. LLDPE/RH composites (a) untreated (b) 1% silane-treated (c) 3% silane-treated (d) 5% silane-treated and (e) 7% silane-treated at dynamic loading loadings

modes were detected such as filler micro buckling. These failure modes were related to composites that have poor, intermediate and high levels of fiber/matrix adhesion [38]. As Canché et al. [39] pointed out, the matrix contributes to the composite strength by avoiding filler bending and buckling because it hinders their ability to bend. Thus, when the matrix starts yielding, the misaligned filler tends to buckle but the matrix surrounding them, after yielding, tends to strain harden and the specimen is capable of carrying more loads. In comparison, composite with optimum 5% treated LLDPE/RH composites recorded the highest thickness after compressed under both static and dynamic, proving that better adhesion of LLDPE/RH resulted in less

deformation experienced by the treated composites. Figure 11 shows the schematic diagram of failure modes generated from experiment run on untreated and treated LLDPE/RH composites tested at both static and dynamic loadings. Interestingly, the images in Figure 9 and Figure 10 show good correlation with the result discussed in Figure 7 and Figure 8. Besides, for dynamic loading, matrix cracking occurs and all the tested composites experience severe catastrophic fracture. To further investigate the fracture behavior, untreated and treated LLDPE/RH composites under dynamic loading will be observed using SEM equipment. The details of the finding have been discussed in the next sub-section.

3.5.2. Fracture Surface Analysis

Figure 12 shows the SEM micrograph of untreated and treated LLDPE/RH composites under 300× magnification of the dynamic compression fracture at a high strain rate loading 1100 s^{-1} of strain. From fractographic analysis, it was observed that the fracture surface of treated composites is relatively smooth compared to untreated composites at dynamic loading, due to the enhancement of the applied stress during high strain rate loading. In this figure, it was observed that untreated LLDPE/RH composite tend to be pulled-out under dynamic loading that causes the presence of holes and voids. The holes and voids did

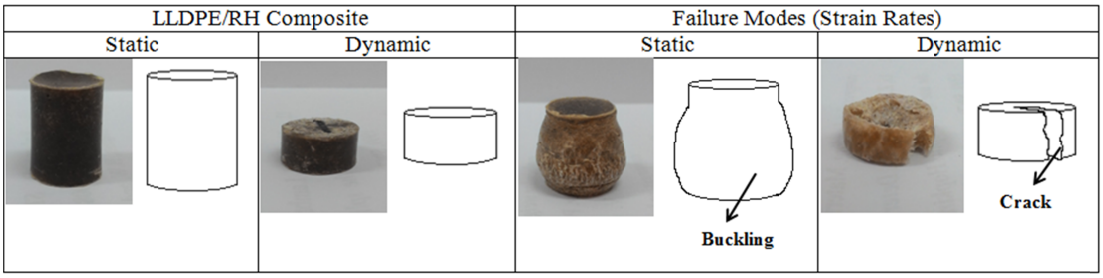

Fig. 11. The schematic diagram of untreated and treated LLDPE/RH composites at static and dynamic loading

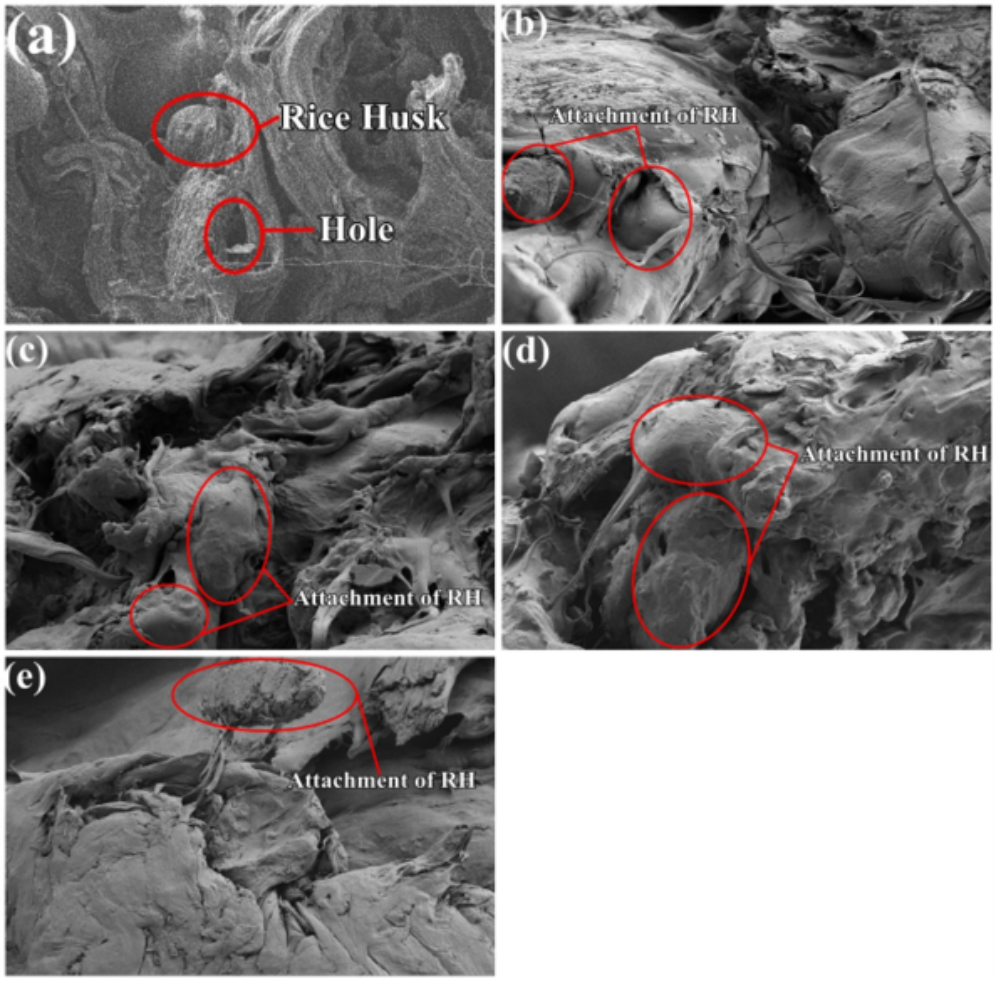

Fig. 12. The fracture structure of LLDPE/RH composites, (A) untreated (B) 1% silane-treated (C) 3% silane-treated (D) 5% silane-treated and (E) 7% silane-treated at dynamic loading

not appear on the fracture surface of the treated LLDPE/RH composites. Besides, the good attachment between the RH and LLDPE was seen under the micrograph. The adhesion between the filler and the matrix was enhanced due to the presence of silane coupling agent in the treated composites.

Theoretically, the better filler-matrix adhesion can be seen when less filler was pulled out, less holes were present and there was a good attachment between the filler and matrix. The adhesion between silane treated RH filler and LLDPE matrices was strong enough so that the filler was rather broken under stress [40]. This observation is in good agreement with the explanation made in Figure 5 and Figure 8, where the treated composites recorded higher UCS and yielded stress compared to untreated composites. Thus, this proves that RH filler treatment with silane coupling agent is effective in enhancing the mechanical properties of LLDPE/RH composites under high strain rates loading.

4. Conclusion

The influence of filler surface modification on the static and dynamic mechanical responses of LLDPE/RH composites was successfully investigated using a conventional universal testing machine and a split Hopkinson pressure bar equipment, up to nearly 1200 s^{-1} of strain rates, respectively. From the overall results, the following conclusions can be drawn:

- The effectiveness of silane treatment on rice husk (RH) particles was successfully confirmed using Field Emission Scanning Electron Microscopy (FESEM) and Fourier Transform Infrared (FTIR).
- Results show that the silane treatment of rice husk (RH) particles gave significant effects on the compressive properties of the LLDPE/RH composites. Quantitatively, treated LLDPE/RH composites (with optimum of 5% silane weight percentage) recorded higher compression properties, in terms of ultimate strength, stiffness yield behaviour, as compared to untreated LLDPE/RH composites.
- Furthermore, it was found that the strain rate sensitivity of both untreated and treated LLDPE/RH composites increased with increasing strain rate, whereas thermal activation values show a contrary trend. Unfortunately, it was recorded that the silane coupling agent does not give any significant trend on the strain rate sensitivity and thermal activation volume of both untreated and treated LLDPE/RH composites.
- From the fracture surface analysis, it was observed that the treated LLDPE/RH composites experienced less permanent deformation compared to its counterpart (untreated LLDPE/RH composites) under static loading. Meanwhile, under dynamic loading, it was observed that untreated LLDPE/RH composites tend to be pulled out (debond) due to poor bonding, and thus, enhance the formation of holes and voids. However, these holes and voids did not appear on the fracture surface of the treated LLDPE/RH composites. Besides, good attachment between rice husk (RH) filler and LLDPE matrix was observed for treated LLDPE composites due to the presence of silane coupling agent.

Acknowledgements

The author would like to acknowledge Malaysian Ministry of Higher Education (MOHE), Fundamental Research Grant (FRGS) (Grant no.: FRGS/2/2013/TK04/UNIMAP/02/2), Universiti Malaysia Perlis (Grant no.: 9003-00390, 9007-00067, 9017-00014, 9007-00130) and Universiti Sains Malaysia (USM) (Grant no.: 811070) for sponsoring and providing financial assistance for this research work. The authors would like to extend their gratitude to Department of Physics and Faculty of Mechanical Engineering and Computer Science, Częstochowa University of Technology, Częstochowa, Poland.

REFERENCES

[1] J.P. Dhal, S.C. Mishra, Processing and Properties of Natural Fiber-Reinforced Polymer Composite. J. Mater. **2013**, 1-6 (2013).

[2] I. Krupa, A. Luyt, Thermal and mechanical properties of extruded LLDPE/wax blends. Polym. Degrad. Stab. **73** (1), 157-161 (2001).

[3] S. Shinoj, R. Visvanathan, S. Panigrahi, N. Varadharaju,. Dynamic mechanical properties of oil palm fibre (OPF)-linear low density polyethylene (LLDPE) biocomposites and study of fibre-matrix interactions. Biosyst. Eng. **109** (2), 99-107 (2011).

[4] A.I. Khalf, A.A. Ward, Use of rice husks as potential filler in styrene butadiene rubber/linear low density polyethylene blends in the presence of maleic anhydride. Mater. Des. **31** (5), 2414-2421 (2010).

[5] S.M. Zabihzadeh, Water Uptake and Flexural Properties of Natural Filler/HDPE Composites. BioResources. **5** (1), 316-323 (2010).

[6] N. Soltani, A. Bahrami, L. González, A Review on the physicochemical treatments of rice husk for production of advanced materials. Chem. Eng. J. **264**, 899-935 (2015).

[7] L. Ludueña, D. Fasce, V.A. Alvarez, P.M. Stefani, Nanocellulose from rice husk following alkaline treatment to remove silica. BioRes. **6** (2), 1440-1453 (2011).

[8] T.P.T. Tran, J.-C. Bénézet, A. Bergeret, Rice and Einkorn wheat husks reinforced poly(lactic acid) (PLA) biocomposites: Effects of alkaline and silane surface treatments of husks. Ind. Crops Prod. **58**, 111-124 (2014).

[9] S.-K. Yeh, C.-C. Hsieh, H.-C.Chang, C.C.C. Yen, Y.-C. Chang, Synergistic effect of coupling agents and fiber treatments on mechanical properties and moisture absorption of polypropylene-rice husk composites and their foam. Compos. Part A Appl. Sci. Manuf. **68**, 313-322 (2015).

[10] M.M. Kabir, H. Wang, K.T. Lau, F. Cardona, Chemical treatments on plant-based natural fibre reinforced polymer composites: An overview. Compos. Part B Eng. **43**, 2883-2892 (2012).

[11] Y. Xie, C.A.S. Hill, Z. Xiao, H. Militz, C. Mai, Silane coupling agents used for natural fiber/polymer composites: A review. Compos. Part A Appl. Sci. Manuf. **41**, 806-819 (2010).

[12] M. Abdelmouleh, S. Boufi, M.N. Belgacem, A. Dufresne, Short natural-fibre reinforced polyethylene and natural rubber composites: Effect of silane coupling agents and fibres loading. Compos. Sci. Technol. **67**, 1627-1639 (2007).

[13] H. Demir, U. Atikler, D. Balköse, F. Tıhmınlıoğlu, The effect of fiber surface treatments on the tensile and water sorption properties of polypropylene-luffa fiber composites. Compos. Part A Appl. Sci. Manuf. **37**, 447-456 (2006).

[14] N.A. Maziad, D.E. El-Nashar, E.M. Sadek, The effects of a silane coupling agent on properties of rice husk-filled maleic acid anhydride compatibilized natural rubber/low-density polyethylene blend. J. Mater. Sci. **44**, 2665-2673 (2009).

[15] H. Ku, H. Wang, N. Pattarachaiyakoop, M. Trada, A review on the tensile properties of natural fiber reinforced polymer composites. Compos. Part B Eng. **42**, 856-873 (2011).

[16] J.O. Agunsoye, V.S. Aigbodion, Bagasse filled recycled polyethylene bio-composites: Morphological and mechanical properties study. Results Phys. **3**, 187-194 (2013).

[17] S.N. Kasa, M.F. Omar, M.M.A. Abdullah, I.N. Ismail, S.S. Ting, S.C. Vac, P. Vizureanu, Effect of Unmodified and Modified Nanocrystalline Cellulose Reinforced Polylactic Acid (PLA) Polymer Prepared by Solvent Casting Method Morphology, mechanical and thermal properties. Mater. Plast. **54** (1), 91-97 (2017).

[18] H. Jaya, M.F. Omar, H.M. Akil, Z.A. Ahmad, N.N. Zulkepli, M.M.A. Abdullah, I.G. Sandu, P. Vizureanu, Effect of Surface Modification on Sawdust Reinforced High Density Polyethylene Composites Under a Wide Range of Strain Rates, Mater. Plast. **53** (1), 85-90 (2016).

[19] G.E. Popita, C. Rosu, D. Manciula, O. Corbu, A. Popovici, O. Nemes, A.V. Sandu, M. Proorocu, S.B. Dan, Industrial Tanned Leather Waste Embedded in Modern Composite Materials. Mater. Plast. **53** (2), 308-311 (2016).

[20] H.S. Kim, B.H. Lee, S.W. Choi, S. Kim, H.J. Kim, The effect of types of maleic anhydride-grafted polypropylene (MAPP) on the interfacial adhesion properties of bio-flour-filled polypropylene composites. Compos. Part A Appl. Sci. Manuf. **38**, 1473-1482 (2007).

[21] M.N. Ichazo, C. Albano, J. Gonzalez, R. Perera, M.V. Candal, Polypropylene/wood flour composites: Treatments and properties. Compos. Struct. **54**, 207-214 (2001).

[22] D.J. Frew, M.J. Forrestal, W. Chen. Pulse shaping techniques for testing brittle materials with a split Hopkinson pressure bar. Exp. Mech. **42**, 93-106 (2002).

[23] F. Hughes, A. Prudom, G. Swallowe, The high strain-rate behaviour of three molecular weights of polyethylene examined with a magnesium alloy split-Hopkinson pressure bar. Polym. Test. **32**, 827-834 (2013).

[24] Z. Li, J. Lambros, Determination of the dynamic response of brittle composites by the use of the split Hopkinson pressure bar. Compos. Sci. Technol. **59**, 1097-1107 (1999).

[25] R. Syafri, I. Ahmad, I. Abdullah, Effect of rice husk surface modification by LENR the on mechanical properties of NR/HDPE reinforced rice husk composite. Sains Malaysiana **40**, 749-756 (2011).

[26] T. Lu, M. Jiang, Z. Jiang, D. Hui, Z. Wang, Z. Zhou, Effect of surface modification of bamboo cellulose fibers on mechanical properties of cellulose/epoxy composites. Compos. Part B Eng. **51**, 28-34 (2013).

[27] A. Valadez-Gonzalez, J.M. Cervantes-Uc, R. Olayo, P.J. Herrera-Franco, Effect of fiber surface treatment on the fiber-matrix bond strength of natural fiber reinforced composites. Compos. Part B Eng. **30**, 309-320 (1999).

[28] M.S. Huda, L.T. Drzal, A.K. Mohanty, M. Misra, The effect of silane treated- and untreated-talc on the mechanical and physico-mechanical properties of poly(lactic acid)/newspaper fibers/talc hybrid composites. Compos. Part B Eng. **38**, 367-379 (2007).

[29] C. Guo, L. Zhou, J. Lv, Effects of expandable graphite and modified ammonium polyphosphate on the flame-retardant and mechanical properties of wood flour-polypropylene composites. Polym. & Polym. Compos. **21** (7), 449-456 (2013).

[30] S. Ifuku, H. Yano, Effect of a silane coupling agent on the mechanical properties of a microfibrillated cellulose composite. Int. J. Biol. Macromol. **74**, 428-432 (2015).

[31] H. Demir, D. Balköse, S. Ülkü, Influence of surface modification of fillers and polymer on flammability and tensile behaviour of polypropylene-composites. Polym. Degrad. Stab. **91**, 1079-1085 (2006).

[32] I. O. Oladele, J.A. Omotoyinbo, J.O.T Adewara, Investigating the Effect of Chemical Treatment on the Constituents and Tensile Properties of Sisal Fibre. *J.* Miner. Mater. Charact. Eng. **9** (6), 569-582 (2010).

[33] C. Parida, S.K. Dash, S.C. Das, Effect of Fiber Treatment and Fiber Loading on Mechanical Properties of Luffa – Resorcinol Composites. Ind. J. Mater. Sci. 2015, 1-6 (2015).

[34] D. Shanmugam, M. Thiruchitrambalam, Static and dynamic mechanical properties of alkali treated unidirectional continuous Palmyra Palm Leaf Stalk Fiber/jute fiber reinforced hybrid polyester composites. Mater. Des. **50**, 533-542 (2013).

[35] I.L. Dubnikova, S.M. Berezina, A.V. Antonov, Effect of rigid particle size on the toughness of filled polypropylene. J. Appl. Polym. Sci. **94**, 1917-1926 (2004).

[36] S.-T. Chiou, W.-C. Cheng, W.-S. Lee, Strain rate effects on the mechanical properties of a Fe–Mn–Al alloy under dynamic impact deformations. Mater. Sci. Eng. A **392**, 156-162 (2005).

[37] M.F. Omar, N.S. Abd Wahab, H.M. Akil, Z.A. Ahmad, M.F.A Rasyid, N.Z. Noriman, Effect of Surface Modification on Strain Rate Sensitivity of Polypropylene/Muscovite Layered Silicate Composites. Mater. Sci. Forum **803**, 343-347 (2014).

[38] L.J. Broutman, Measurement of the Fiber-Polymer Matrix Interfacial Strength. In Interfaces in Composites, ASTM STP 452, 27-41 (1969).

[39] G. Canché-Escamilla, J. Rodriguez-Laviada, J.I. Cauich-Cupul, E. Mendizábal, J.E. Puig, P.J. Herrera-Franco, Flexural, impact and compressive properties of a rigid-thermoplastic matrix/cellulose fiber reinforced composites. Compos. - Part A Appl. Sci. Manuf. **33**, 539-549 (2002).

[40] R. Santiagoo, H. Ismail, K. Hussin, Mechanical properties, water absorption, and swelling behaviour of rice husk powder filled polypropylene/recycled acrylonitrile butadiene rubber (PP/NBRr/RHP) biocomposites using silane as a coupling agent. BioRes. **6** (4), 3714-3726 (2011).